Investigation of the hydration process of a wollastonite-based brushite cement

C. Cau Dit Coumes, P. Laniesse, Adel Mesbah, G. Le Saout, P. Gaveau, G. Silly

Investigation of the hydration process of a wollastonite-based brushite cement

Cau Dit Coumes, C. [1], Laniesse, P.[1], Mesbah, A.[2], Le Saout, G.[3], Gaveau, P.[4], Silly, G.[4]

[1] CEA, DEN, Univ. Montpellier, DE2D, SEAD, LCBC, F-30207 Bagnols-sur-Cèze cedex, France

[2] ICSM, UMR 5257 CEA / CNRS / UM / ENSCM, Site de Marcoule – Bât. 426, BP 17171, 30207 Bagnols-sur-Cèze cedex, France

[3] Centre des Matériaux des Mines d'Alès (C2MA), Ecole des Mines d'Alès (Institut Mines Telecom), Avenue de Clavières 6, 30100 Alès cedex, France

[4] Institut Charles Gerhardt de Montpellier, UMR 5253, CNRS UM ENSCM, Montpellier 34095, France

Abstract

Wollastonite-based brushite cements are mainly used for refractory material applications, but they may also offer new prospects for the solidification/stabilization of hazardous wastes. Most studies on these binders have been focused on the characterization of the final products, on the associated microstructure or on the functional properties of the resulting materials. This work provides new insight into their setting and hardening process, by characterizing the evolution of both the liquid and solid phases with ongoing hydration.

The investigated binder was a two-component system, consisting of wollastonite and of a phosphoric acid solution containing borax and metallic cations (Al^{3+}, Zn^{2+}). The hydration process was investigated using a cell allowing the simultaneous measurement of the elastic modulus and the electrical conductivity during setting. The phase assemblage was characterized by X-ray diffraction, scanning electron microscopy and ^{31}P and ^{27}Al MAS-NMR.

Hydration was a multi-step process which yielded several products: amorphous silica, monocalcium phosphate monohydrate ($Ca(H_2PO_4)_2.H_2O$) which precipitated transiently during the first stage of hydration, and brushite (CaHPO4.2H2O) which crystallized at higher pH. In addition, elemental mapping by SEM-EDS showed the precipitation of an amorphous phase containing phosphate, aluminum and zinc, which tended to get richer in calcium with ongoing hydration. Its structure was investigated by NMR spectroscopy (one pulse ^{31}P and ^{27}Al and REDOR $^{27}Al/^{31}P$). It mainly contained hexavalent aluminum bonded to orthophosphate moieties. This amorphous phase was shown to play a key role in the consolidation process of the material and its final strength.

1. INTRODUCTION

During the decommissioning of old nuclear facilities, cleaning operations can produce acidic waste streams which have to be stabilized and solidified before their final disposal. Portland cement is extensively used for the conditioning of low- or intermediate-level radioactive wastes. However, its high alkalinity is a serious obstacle in the case of acidic waste. Indeed, an exothermic acid-base reaction occurs between the highly acidic waste and hydroxide ions released by the dissolution of cement phases, resulting in significant temperature rise and flash setting of the grout. The waste thus needs to be neutralized, at least to some degree, prior to cementation. This pre-treatment step has several drawbacks.*(i)* The final volume of the waste to be cemented is increased.*(ii)* Neutralization of the waste causes the precipitation of flocs of metallic hydroxide (aluminum, iron, zinc, uranium…). A significant amount of water can be bound to the floc particles and is unavailable to contribute to workability, explaining why a floc / cement paste can be highly viscous despite its high water content (Collier, 2009). *(iii)* When the pre-treatment reagent is a concentrated sodium or potassium hydroxide, significant amounts of alkalis are added to the waste, and thus to the cement-waste forms, with

possible deleterious effects in the long term (such as the formation of a gel-like product due to alkali-aggregate reaction (Stanton, 1940)).

This study aims at investigating phosphate binders which may show an improved chemical compatibility with acidic wastes, as compared to usual calcium silicate cements. Phosphate binders are often referred as “chemically bonded phosphate ceramics” because they can produce materials with very low porosity and high mechanical strength (Wagh, 2002). Their setting and hardening result from the precipitation of crystallized hydrates with low solubility, often associated with poorly characterized amorphous phases. This work is focused on a brushite cement prepared from wollastonite ($CaSiO_3$), a natural calcium meta-silicate, and phosphoric acid (H_3PO_4), as firstly described by Semler (Semler, 1976). The reaction starts in very acidic medium (pH close to zero), but the pH increases rapidly to reach equilibrium at a value close to 6 (Semler, 1976). For P/Ca molar ratios between 0.39 and 1, the sole precipitated calcium phosphate is brushite (CaHPO4•2H2O). Amorphous silica is also formed according to balance reaction (1) (Semler, 1976).

$$CaSiO_3 + H_3PO_4 + (1+x)\ H_2O \rightarrow SiO_2{\bullet}xH_2O + CaHPO_4{\bullet}2H_2O \quad (1)$$

The objective of this work is to provide a deeper understanding of the setting and hardening process by using a robust methodology previously developed with success to investigate hydration of calcium sulfoaluminate and silicate cements (Champenois, 2013).

2. EXPERIMENTAL

2.1 Materials and specimen preparation

The wollastonite-based binder was provided by Sulitec under the trade name of Fotimine. It was a two-component system comprising:

- a powder containing wollastonite (98.4 wt.%) and calcite (1.6 wt.%),
- a phosphoric acid solution (9 mol/L), containing metallic cations (Al^{3+}, Zn^{2+}) (1.3 mol/L) and borax (0.15 mol/L) as a retarding agent.

The weight ratio of the mixing solution to the cement powder was fixed to 1.25 in all samples, resulting in a Ca/P molar ratio of 1.2. Mixing was performed during 5 min using a laboratory mixer equipped with an anchor stirrer and rotating at 250 rpm. Some paste samples were cast into airtight polypropylene boxes (20 mL of paste per box), and cured at 25 ± 1°C.

Additional cement pastes were prepared using the same ratios by mixing the powder with a phosphoric acid solution (9 mol/L) containing Al^{3+} and borax in variable concentrations, as shown in Figure 1. 4x4x4 cm plugs were cast and cured for 28 d in sealed bag at room temperature (21 ±1 °C).

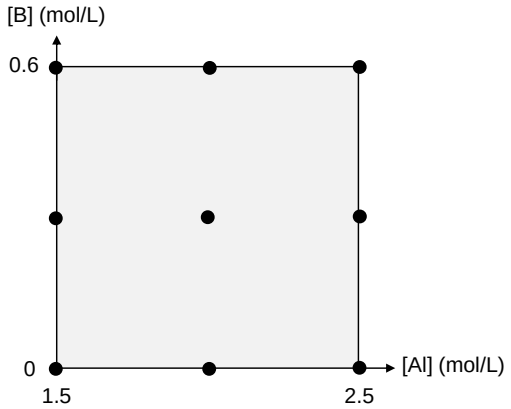

Figure 1. Selected experimental design: investigated concentrations of Al and B in the mixing solution.

2.2 Characterization techniques

The hydration process was followed by monitoring the viscoelastic properties and the electrical conductivity of the paste with ongoing hydration, using a specifically designed device (Champenois, 2013). The cell, cylindrically shaped with two annular stainless steel electrodes, was thermostated at 25°C by circulation of cooling water in a double envelope. It was connected to an electrochemistry meter (Consort C 861) with a BNC cable, to collect electrical conductivity data. The conductivity cell was calibrated using a 12.888 mS/cm standardized KCl solution at 25°C. Evolution of the viscoelastic properties of the paste was followed by dynamic mode rheometry using a strain-driven controlled stress rheometer (AR-G2 TA Instrument, USA). A sinusoidal shear strain (γ) was applied to the cement paste at constant frequency (ω). The resulting stress (τ) was measured via a torque and was also sinusoidal with a δ phase lag with respect to the applied strain. In order to stay in the linear viscoelasticity domain of the materials, and thus to avoid destructive measurement, experiments were performed using a 10^{-4} shear strain and a 1 rad/s frequency. The ratio between the stress and the shear strain was equal to the complex modulus G* defined as:

$$G^* = G' + iG'' \quad (2)$$

with G' the shear storage or elastic modulus and G'' the shear loss or viscous modulus. A specific minivane geometry (stainless steel, radius of 20 mm, length of 3 cm, K_γ = 2.479 and K_σ = 42050 cm^{-3}) was used to perform all the experiments.

Cement hydration was also stopped after fixed periods of time by successively immersing the crushed paste into isopropanol and drying it in an oven at 38°C for 24 h. The phase assemblage of samples aged from 30 min to 48 h was characterized by X-ray diffraction using the Debye-Scherer configuration (transmission mode) (PanAlytical X'pert Pro, copper anode, $\lambda_{K\alpha1}$=1.54056 Å, 45 mA and 40 kV, scanning from 2θ = 5° to 120° in 0.017° steps, for a total counting time of 6 h). Powders were ground by hand at a particle size below 80 µm and mixed with 10 wt.% of silicon used as an external standard for quantitative analysis. Fullprof_suite software was used for semi-quantitative analysis of the different phases with the Rietveld method (Frontera, 2003). The Rietveld calculation provided the weight fraction of each crystalline phase and of the total amorphous phases.

Since hydration not only consumed water but also aqueous phosphate, aluminium and zinc species, quantitative elemental analysis of the paste samples was also performed in order to calculate the mass of each phase over time. The samples were first submitted to solid digestion in lithium metaborate (to quantify Ca, Al, Zn, P, Na and Si) and in sodium carbonate (to quantify B), and then analysed by ICP-AES. Analyses of the pore solution (not shown here) revealed that the dissolved silicate concentration was negligible. Thus, the total mass of solid phase at time *t* was given by equation 3:

$$m_s(t) = m(Si)_0 / \%Si(t) \quad (3)$$

with $m(Si)_0$ the initial mass of silicon and %Si(t) the weight fraction of silicon in the solid phase determined by ICP-AES. Knowing the mass of solid for a given hydration time, the masses of each phase were calculated using the weight fractions determined by Rietveld analysis. Then, the amount of amorphous silica was assessed by subtracting the amount of silica in wollastonite and in quartz from the total amount of silica. Finally, the amount of aluminum, calcium, phosphorus and zinc in amorphous phase(s) were calculated by mass balance.

The paste samples were also characterized by ^{31}P and ^{27}Al MAS NMR spectroscopy. Spectra were recorded on a Bruker Avance 600 NMR spectrometer (field strength of 14.1 T) applying 20 kHz spinning rate on a 3.2 mm CP MAS probe using ZrO_2 rotors. ^{31}P and ^{27}Al MAS NMR spectra were recorded at 242.86 MHz and 156.29 MHz respectively. Single-pulse experiments were carried out by applying 90° pulses decoupling and recycle delays of 240 s for ^{31}P spectra and of 1 s for ^{27}Al spectra. The ^{31}P and ^{27}Al chemical shifts were referenced externally with respect to K_2HPO_4 (4.1 ppm) and $Al(NO_3)_3$ solutions respectively.

The chemical environment of Al nuclei was characterized employing $^{27}Al\{^{31}P\}$-REDOR (Rotational Echo Double Resonance) NMR. This technique, which combines magic angle spinning with rotor-synchronized radiofrequency pulses, is interesting in interpreting spectra of nuclei with magic spin quantum number I = ½ (e.g. ^{31}P) that are coupled via heteronuclear dipolar interactions to quadrupolar nuclei (e.g. ^{27}Al).The objective of the pulse sequence was to obtain, for each rotor period, one spectrum which was not affected by Al/P coupling, as in classical MAS-NMR analysis, and one which was affected by this coupling if it exists (Gullion, 2008). Between two sets of pulse sequences, the number of rotor rotations was incremented from 1 to 39 with a step of 2. The first pulse sequence was a classical ^{27}Al ECHO sequence and the second one a ^{27}Al ECHO sequence with a π pulse on ^{31}P in the middle of the ECHO time (Chan, 2000).

The compressive strength of hardened paste samples was measured on 4x4x4 cm plugs following European standard EN 196-1.

3. RESULTS AND DISCUSSION

3.1 Description of the hydration process

The evolution of the elastic modulus and electrical conductivity of the cement paste during the first 48 h after mixing is shown in Figure 2. The hydration process could be divided into three steps according to the rheometric measurements.

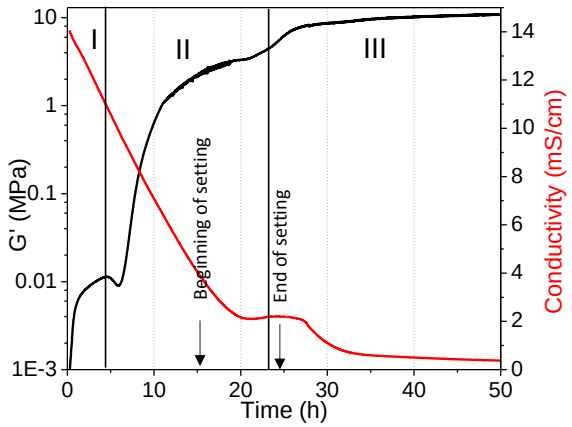

Figure 2. Evolution of elastic modulus and electrical conductivity with ongoing hydration.

During the first stage of hydration (0 to 4 h), the elastic modulus exhibited a first rise, while the electrical conductivity started to decrease, which could be explained by a decrease in the acidity of the interstitial solution (dissolution of wollastonite consuming H^+ ions according to reaction (4)) and by the precipitation of the first hydrates.

$$CaSiO_3 + 2H^+ + xH_2O \rightarrow Ca^{2+} + SiO_2.(x+1)H_2O\ (am) \quad (4)$$

The mineralogical evolution inferred from the XRD patterns (Figure 3) showed a slight dissolution of wollastonite, with precipitation of traces of crystalline monocalcium phosphate monohydrate (MCPM: $Ca(H_2PO_4)_2.H_2O$) and of large amounts of an amorphous phase containing phosphate, aluminum and zinc. Its Ca/P, Al/P and Zn/P molar ratios, determined by SEM-EDS after 30 min of hydration, were 0.13 ± 0.06, 0.28 ± 0.05 and 0.22 ± 0.04 respectively. Such kind of phase has already been reported for zinc phosphate dental cement (Jabri, 2012), but has never been fully characterized. Its stoichiometry, assessed from mass balance calculations and Rietveld analysis, was $(ZnO)_{0.20\pm0.03}(Al_2O_3)_{0.12\pm0.04}(P_2O_5)_{1.0\pm0.1}.xH_2O$. The Zn/P and Al/P ratio were in rather good agreement with those determined by EDS analysis. However, the calculated composition was free of calcium whereas this element was detected in small amount by EDS analysis. Two hypotheses could explain these contradictory results: *(i)* the amorphous phase actually contained small amounts of calcium which were not evidenced by mass balance calculation due to experimental uncertainties, *(ii)* the calcium

detected by EDS analysis was due to intermixing at the submicronic level of the amorphous phase with other calcium-containing minerals (wollastonite, MCPM).

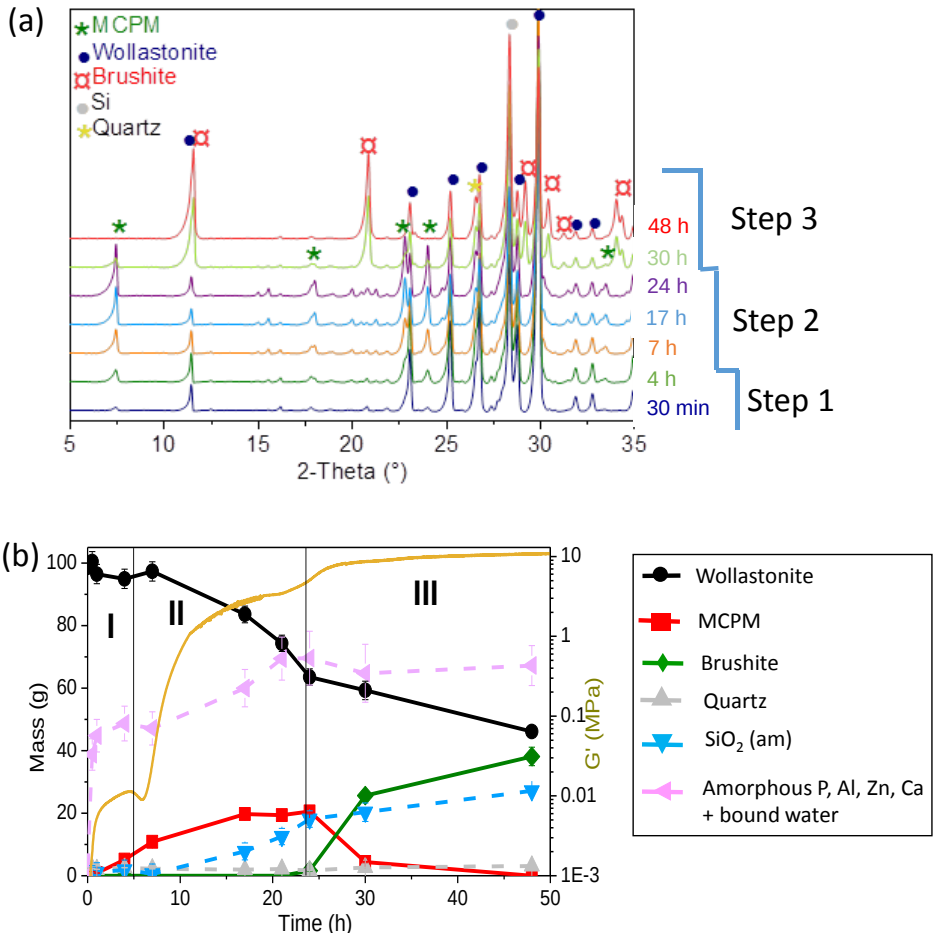

Figure 3. XRD patterns (a) and phase evolution (b) with ongoing hydration.

During the second step (4 to 24 h), the elastic modulus exhibited a second rise up to 3 MPa, meaning that the paste started to consolidate (the beginning of setting, measured using a Vicat needle, occurred during this period), while the electrical conductivity went on decreasing. Wollastonite dissolved more rapidly, forming amorphous silica (incongruent dissolution) and significant amounts of MCPM. The amorphous phase precipitated more slowly than in step 1 and it tended to get richer in calcium, as shown by the evolution of its Ca/P molar ratio determined by EDS analysis (Figure 4).

During the third period (after 24 h), the electrical conductivity first remained constant (2 mS/cm), and then decreased again, while the elastic modulus exhibited a third rise, corresponding to the end of setting. Wollastonite continued to dissolve. MCPM was destabilized during this period and brushite precipitated. As for the amorphous phosphate phase, it did not evolve notably during this stage. Its stoichiometry, derived from mass balance calculations, was $(ZnO)_{0.19\pm0.03}(Al_2O_3)_{0.11\pm0.04}(CaO)_{0.4\pm0.2}(P_2O_5)_{1.0\pm0.2}.yH_2O$ at 48 h. The transient levelling-off of the electrical conductivity could be explained by the occurrence of two antagonistic processes:

- conversion of MCPM into brushite which released H^+ and $H_2PO_4^-$ ions in solution (reaction (5));

$$Ca(H_2PO_4)_2.H_2O + H_2O \rightarrow CaHPO_4.2H_2O + H^+ + H_2PO_4^- \quad (5)$$

- dissolution of wollastonite which continued to consume H^+ ions (reaction (4)).

Its final drop at a value close to zero was mainly explained by the loss of mobility of the ionic species in the pore solution due to the setting and hardening of the material.

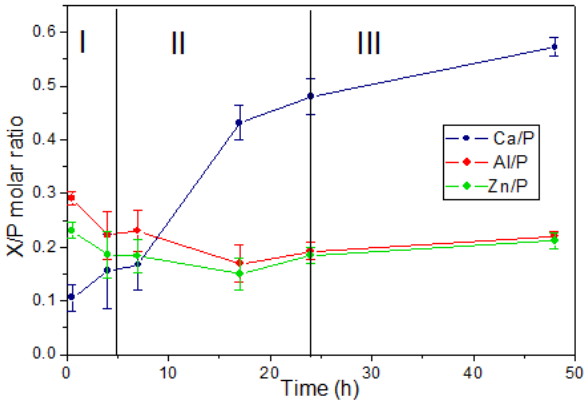

Figure 4: Evolution of the Ca/P, Al/P and Zn/P molar ratios (determined by SEM-EDS analysis) of the amorphous phosphate phase.

3.2 NMR characterization of the amorphous phase

^{31}P and ^{27}Al MAS-NMR spectra were recorded on a 30 min-old-sample (Figure 5, Figure 6). The ^{31}P NMR spectrum showed the presence of MCPM (peaks at 0.1 and -4.3 ppm (Legrand, 2009)), but also of one or several other phosphate minerals (resonances at-1.3, -6.7 and -12.5 ppm). In addition, the ^{27}Al spectrum showed the presence of a peak at -14.1 ppm, characteristic of six-fold coordinated aluminum bound to orthophosphate moieties(Al-$(PO)_6$) (MacKenzie, 2002). Therefore, ^{27}Al and ^{31}P NMR experiments suggested the formation of an alumino-phosphate phase at the beginning of hydration, which is in agreement with the conclusions drawn from Rietveld and ICP-AES analyses.

At 48 h, the ^{31}P MAS NMR spectrum showed a sharp peak characteristic of brushite at 1.4 ppm (Legrand, 2009), but other contributions were still noticed at -1.4 and -4.4 ppm. The ^{27}Al MAS NMR spectrum still showed the presence of octahedral aluminum bound to orthophosphate moieties. However, the resonance peak was shifted to less negative chemical shifts (from -14.1 ppm at 30 min to -8.7 ppm at 48 h). This shift revealed a change in the environment of Al-$(PO)_x$ between 30 min and 48h, which could be attributed to the enrichment of the amorphous phase in calcium.

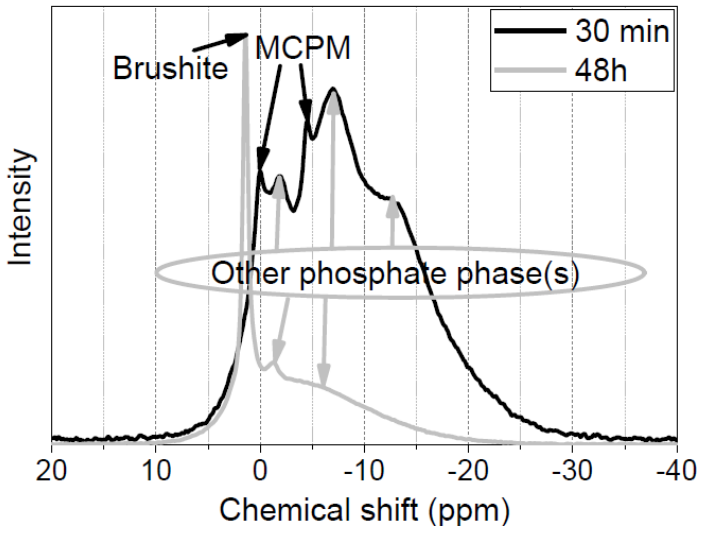

Figure 5. ^{31}P MAS-NMR spectra of the 30 min- and 48 h-old samples.

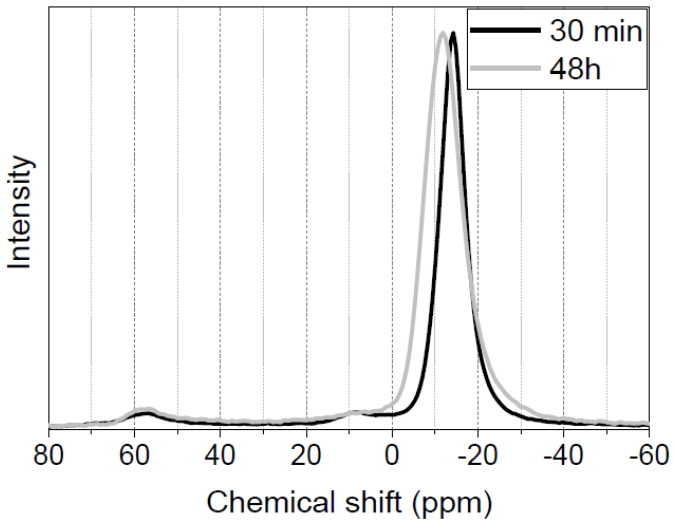

Figure 6. ^{27}Al MAS-NMR spectra of the 30 min- and 48 h-old samples.

^{27}Al{^{31}P} REDOR experiments were performed on the 30 min- and 48 h-old samples to probe the environment of aluminum and its spatial proximity with phosphorus in the amorphous phase. The REDOR curves are shown in Figure 7. They overlaid, meaning that the coupling of aluminium to phosphorus nuclei was the same at both hydration times. Note that the fluctuations observed for the 30 min-old sample curve were due to a bad signal/noise ratio.

The experimental curves of the cement paste samples were then compared to those of reference samples with known crystallographic structure: VPI-5 (experimental curve); $AlPO_4$ and $Al(PO_3)_3$ (Chan *et al.*, 2000). VPI-5 is an aluminophosphate zeolithe ($Al_3(PO_4)_3.7H_2O$) with three types of Al environments (Cheetham *et al.*, 1996): two corresponding to Al in coordination IV coupled to 2 P and one assigned to Al in coordination 6 coupled to 4 P (Figure 8). In this study, we were only interested in the last type of Al nuclei. As for $AlPO_4$ and $Al(PO_3)_3$, they contain only sixfold-coordinated Al coupled to 6 P. The curves relative to the cement paste samples and to VPI-5 overlaid, indicating the same Al environment regarding phosphorus nuclei in these materials. Therefore, the amorphous aluminophosphate phase of the cement paste contained 6-fold coordinated aluminium coupled to 4 P nuclei.

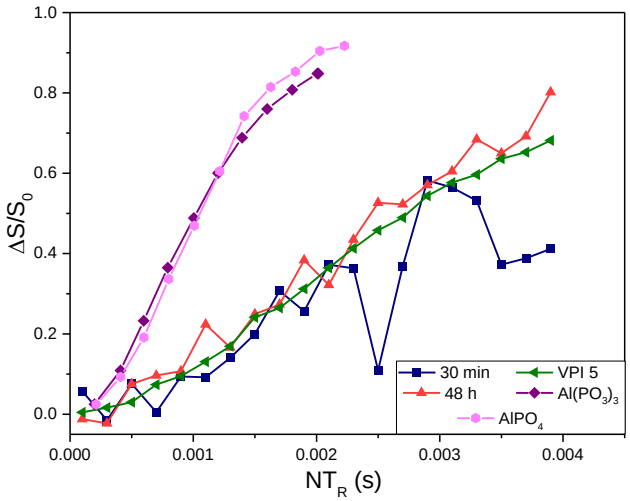

Figure 7. ^{27}Al {^{31}P} REDOR curves of the 30 min- and 48 h-old samples compared to those of reference compounds.

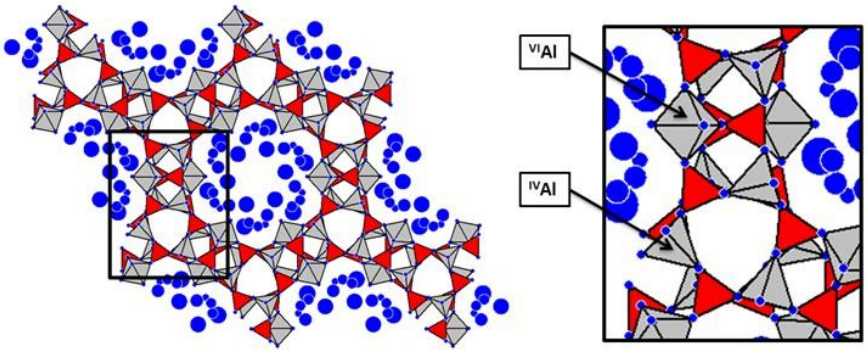

Figure 8. VPI-5 crystalline structure.

3.3 Influence of the amorphous phase on the mechanical properties of the cement paste

To investigate the influence of the amorphous aluminophosphate phase on the properties of the hardened cement paste, twelve samples were prepared with mixing solutions containing variable concentrations of Al^{3+} and borax. Their phase assemblage was determined using Rietveld refinement after 28 d of curing in sealed bag at room temperature (Table 1).

Table 1. Mineralogical composition and compressive strength of the 28 d-old cement pastes.

Concentration in the mixing solution		Phase fraction (wt.%) at 28 d			Compressive strength (MPa)
$[Al^{3+}]$ (mol/L)	[B] (mol/L)	Wollastonite	Brushite	Amorphous aluminophosphate	
1.5	0.2	10.4	52.9	12.5	30.6
2.5	0.2	10.1	343	31.5	57.5
1.5	0.6	17.2	55.3	6.6	35.6
2.5	0.6	17.7	35.5	26.5	55.8
1.5	0.4	15.7	51.9	10.9	30.8
2.5	0.4	14.7	35.2	28.3	47.7
2.0	0.2	12.0	47.8	16.7	40.5
2.0	0.6	15.3	43.4	19.6	45.6
2.0	0.4	15.2	50.3	12.5	45.5
2.0	0.4	12.2	45.8	18.7	36.5
2.0	0.4	11.0	41.0	24.4	461
2.0	0.4	12.7	47.9	16.4	43.9

All the samples contained approximately the same amount of residual wollastonite (13.7 ± 2.7 wt.%). As expected, increasing the initial concentration of aluminium in the mixing solution promoted the formation of the amorphous phase at the expense of brushite (Figure 9). Figure 9-c shows that it also improved greatly the compressive strength.

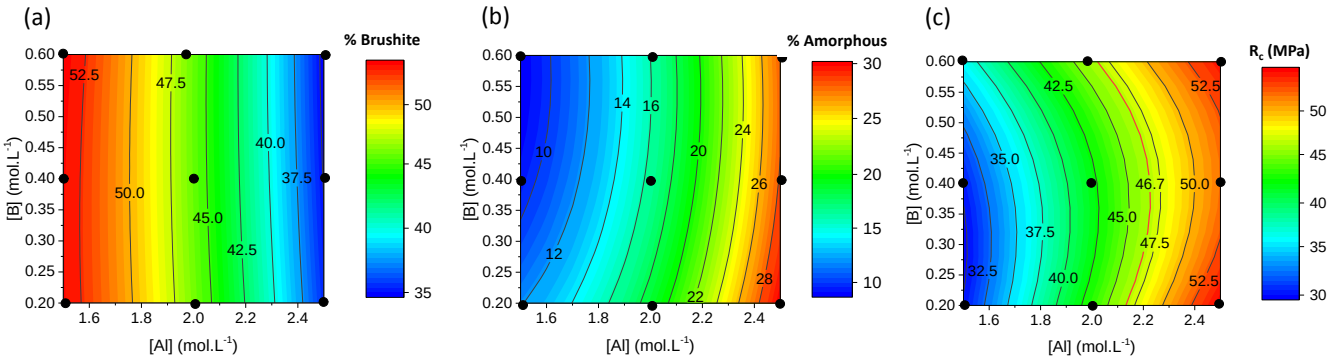

Figure 9. Influence of the B and Al initial concentrations in the mixing solution on the weight fractions of brushite (a) and amorphous phase (b) in the 28-d old cement pastes, as well as on their compressive strength (c).

SEM observations performed on polished sections of the 28 d-old cement pastes revealed a much denser microstructure of the samples prepared with the highest Al concentration in their mixing solution, and thus containing the highest fraction of amorphous phase. This explained their better mechanical properties (Figure 10).

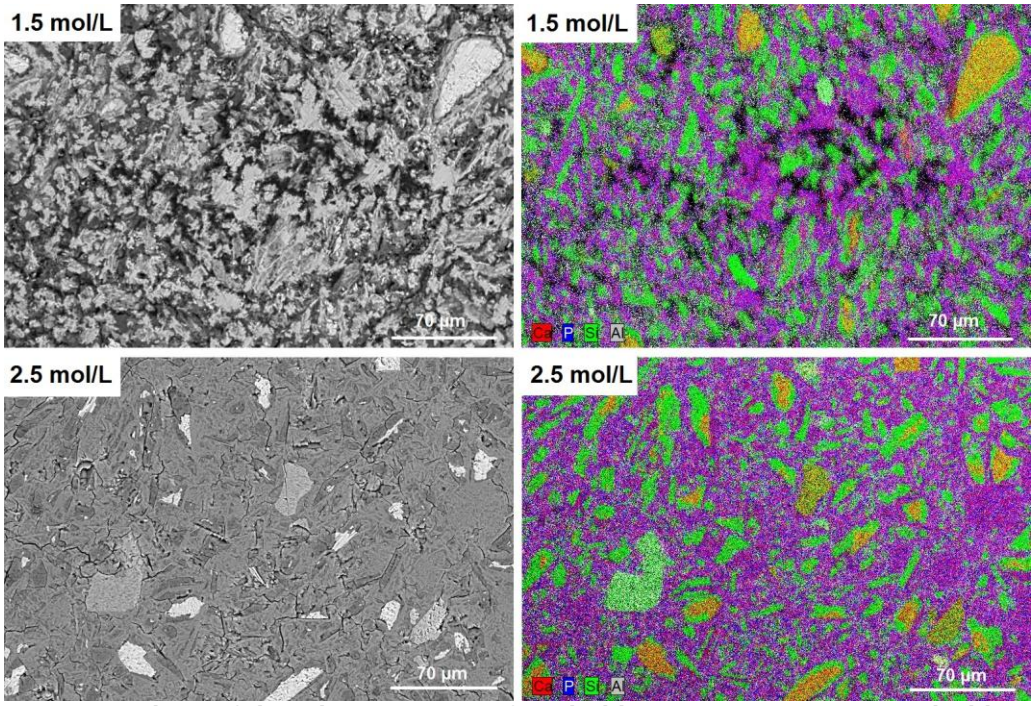

Figure 10. Comparison of the microstructure of 28 d-old cement pastes prepared with a mixing solution containing 1.5 or 2.5 mol/L of Al^{3+} ([B] = 0 mol/L): BSE images (left) and elemental mapping (right).

4. CONCLUSION

This work led to the following conclusions:

1. The reaction of wollastonite with a phosphoric acid solution containing aluminum, zinc and borax is a three-step process.

2. Monocalcium phosphate monohydrate is formed transiently before brushite.

3. An amorphous phosphate phase containing aluminum, zinc and calcium precipitates at early age. This phase tends to get richer in calcium with ongoing hydration. However, the environment of

aluminum nuclei regarding phosphorus nuclei (6-fold coordinated Al coupled to 4 P) remains unchanged between 30 min and 48 h of hydration.

4. Increasing the amorphous fraction of the cement paste greatly improves its compressive strength.

5. REFERENCES

Chan JCC, & Eckert H, *Dipolar Coupling Information in Multispin Systems: Application of a Compensated REDOR NMR Approach to Inorganic Phosphates*. J. Magnetic Resonance 147 (2000) 170-178.

Cheetham G, & Harding MM (1996). *VPI-5: Structure refinement with single crystal synchrotron radiation diffraction data*. Zeolites 16: 245-248.

Chan J.C, Eckert H. (2000) *Dipolar coupling information in multispin systems: application of a compensated REDOR NMR approach to inorganic phosphate*s. J. Magnetic Resonance. 17: 170-178.

Champenois J-B, Cau Dit Coumes C, Poulesquen A, Le Bescop P, & Damidot D (2013). *Beneficial use of a cell coupling rheometry, conductimetry, and calorimetry to investigate the early age hydration of calcium sulfoaluminate cement*. Rheol.Acta, 52: 177-87.

Collier NC, Milestone NB, Hill J, & Godfrey H (2009). *Immobilisation of Fe Floc: Part 2, Encapsulation of floc in composite cement.* J. Nucl. Mater., 393: 92-101

Frontera C, & Rodriguez-Carvajal J (2003). *FullProf as a new tool for flipping ratio analysis*. Physica B, 335: 219 -222.

Gullion (2008). *Rotational-Echo, Double-Resonance NMR*, in: Webb (Ed.) Modern Magnetic Resonance, Springer, pp. 713-718.

Jabri M, Mejdoubi E, El Gadi M, & Hammouti B (2012). *Optimisation of hardness and setting time of dental zinc phosphate cement using a design of experiments*. Arabian J. Chem., 5: 347-51.

Legrand AP, Sfihi H, Lequeux N, & Lemaitre J (2009). *(31)P Solid-State NMR study of the chemical setting process of a dual-paste injectable brushite cements*, J. Biomed. Mater. Res. Part B: Appl. Biomater., 91: 46-54.

MacKenzie, & Smith (2002). *Multinuclear Solid-State Nuclear Magnetic Resonance of Inorganic Materials*, 1 ed., Pergamon Materials Series, Elsevier Science Ltd, Oxford (UK).

Semler CE (1976). *A quick-setting wollastonite phosphate cement*, Ceram. Bull., 55(11): 983-988

Stanton TE (1940). *Expansion of concrete through reaction between cement and aggregate*. Proc. Amer. Soc. Civil Engineers, 66: 1781-1811.

Wagh AS (2004). *Chemically bonded phosphate ceramics: twenty first century materials with diverse applications.* Elsevier Science Ltd*,* Oxford (UK).